Sensitivity and sensing speed analysis of extended nano-cavity and source over electrode in Si/SiGe based TFET biosensor

Anil Lodhi[1] · Chithraja Rajan[1] · Amit Kumar Behera[1] · Dip Prakash Samajdar[1] · Deepak Soni[1] · Dharmendra Singh Yadav[2]

Abstract

In this manuscript, a new approach has been presented to enhance biosensor sensitivity and sensing speed by altering the mobility of charge carriers in the source region. The presented biosensor has been named as hetero material, source electrode tunnel FET, HM-SE-TFET. For comparison, we have considered P^+(Source) N(Channel) N^+(Drain) type architecture. In the proposed device, doped SiGe is used to enhance the mobility of charge carriers in the source region. Additionally, an extra negative biased source electrode is deposited over the source region, which overcomes the material solubility limit. The extra negative biased source electrode attracts the holes from bulk P^+ source which increases the abruptness at the source-channel interface. The increased abruptness at the junction increases the ON State driving current. Further, the cavity which was earlier under the gate electrode has been extended to the source region, which provides a large area to accommodate in the cavity and changes the electrostatic characteristics of the device. Hence the combined effect of hetero material (SiGe) in the source region and extension of cavity to the source region enhances the sensitivity and sensing speed of the biosensor. The effectiveness of the proposed biosensor has been compared with the conventional Si-based TFET biosensor in terms of drain current and device sensitivity.

Keywords Cavity · Biosensing application · Hetero material · Dielectric · Charge density · Sensitivity · Biosensor

✉ Anil Lodhi
  lodhianil011@gmail.com

  Chithraja Rajan
  rajan.chithraja@gmail.com

  Amit Kumar Behera
  amitiiit12@gmail.com

  Dip Prakash Samajdar
  dipprakash010@gmail.com

  Deepak Soni
  deepaksoni09@gmail.com

  Dharmendra Singh Yadav
  dsyadav@nith.ac.in

[1] PDPM Indian Institute of Information Technology, Design and Manufacturing, Jabalpur, Madhya Pradesh, India

[2] National Institute of Technology, Hamirpur, Himachal Pradesh, India

1 Introduction

With the discovery of label-based biosensor, ion-sensitive field effect transistor (ISFET) came into the picture in 1970 which became very popular for detecting charged biomolecule species. But soon its popularity fades away as it has a serious drawback of detecting only one category of biomolecule i.e.charged biomolecules while the neutral biomolecules are left undetected [1–5]. Then, the idea of a label-free biosensor came into existence in which bio-detection potentiality is integrated into established semiconductor technology. A cavity is created in the oxide region under the gate electrode of conventional MOSFET and when the biomolecule is placed in that cavity either dielectric constant changes or the charge density in the cavity changes which in turn changes the drain current of the MOSFET as the gate to channel coupling changes [6–8]. The MOSFET which has been a dominating device for IC Industry has a serious issue of leakage current and high subthreshold slope. Further to this, it has also issued regarding its scalability as short channel effect

(SCEs) and drain induced barrier lowering (DIBL) comes into the picture. The leakage current strongly hampers the biosensor performance as it interferes with the conduction current and increases the percentage error of detection of the biomolecule. Further high SS degrades the response time of the biosensor [9–12]. With the advancement of technology, the demand for efficiency has increased many folds. Hence there is a need to switch to some other device that can overcome these challenges. For this band to band tunneling(BTBT) phenomenon based Tunnel FET has proved to be a promising device for biosensing application as it has very low parasitic current to the order of 10^{-17}, subthreshold swing (SS) < 60 mV/decade and compatible with the existing CMOS technology [8]. The sensing capability of TFET is many folds better than the existing MOSFET technology [13–18]. To improve the sensitivity and sensing speed of the biosensor with the idea of nano-cavity has been proposed in the conventional tunnel FET (C-TFET) biosensor [10]. When biomolecules are introduced into the cavity the coupling strength between gate/channel increases. TFET which is properly known for better scalability without suffering from SCE with low SS and leakage [19–22]. Therefore, biomolecules in cavity changes the coupling between gate electrode and channel which leads to the better band to band tunneling current through bandgap modulation. Higher the current stronger will be the sensor sensitivity for better actuation. The whole concept is revolving around bandgap modulation which depends on the abrupt change in carrier concentrations at source/channel junction. This abruptness is restricted by maximum physical doping absorbed upto Silicon solubility limit [23]. Therefore, it is better to adopt bandgap modulation through hetero material engineering [24] where a low bandgap material at source and a high bandgap material at drain/channel provides steeper band bending leads to high current flow for low supply voltage. In addition, in accordance of our work in [23], an additional negative electrode over source creates a hole plasma layer which enhance source-channel abruptness. Therefore, in this paper a novel Si/SiGe based Hetero Material Source Electrode TFET (HM-SE-TFET) is proposed for highly sensitive and rapid biosensing applications. In addition, there is an extended cavity at source and gate regions where dielectric change through various biomolecule coupling cause a drastic improvement in sensing behavior. The performance of HM-SE-TFET is compared with a C-TFET which showcase that both source electrode and use of hetero-material results in reduced tunneling width at the source-channel junction which inflates the tunneling current and sensing behavior. In the present investigation, the effect of different dielectric materials and different charge densities on the various performance of biosensor

is carried out. The performance is measured on the basis of output drain current, sensitivity and response time.

2 Device structure and simulation setup

This section of the manuscript describes the structure of both conventional and proposed biosensor. Figure 1 shows the cross-sectional view of (a) C-TFET biosensor and (b) HM-SE-TFET biosensor. For both the devices, the design parameters considered are shown in Table 1. The proposed structure is motivated from the quasi-planar FinFet [25–27] technology through which multi-terminal fins can be constructed over a BOX which isolate many substrate related issues such as lower parasitic capacitance, non latchup effect, low leakage current and radiation hardened [26–28]. For the time being, we have neglected less significant substrate issues in biosensing applications and our main focus is the sensitivity and speed improvement of the device towards the biomolecules. The term quasi-planar here indicates that there is some vertical current flow with the current along the plane [25]. So, our device follows
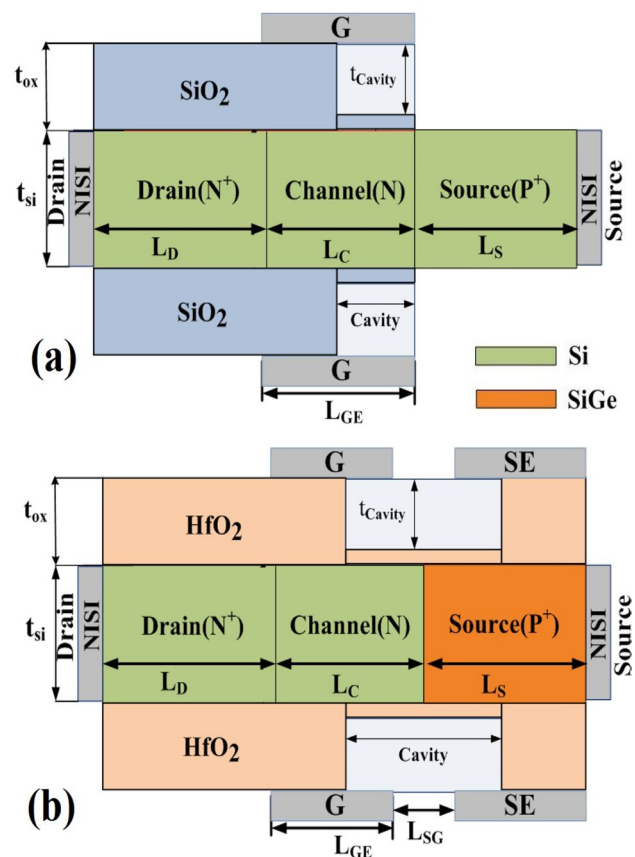
Fig. 1 Schematic view of **a** C-TFET (conventional) and **b** proposed physically doped, Hetero-Material-source electrode tunnel field effect transistor (HM-SE-TFET)

a planar friendly CMOS technology. Other than that, we have a SiGe source and Si drain channel, the fabrication steps for the Si/SiGe bandgap engineered Tunnel FET has been discussed and patented by Zhu et al. [29] in planar bulk technology. For the simulation purpose, the Silvaco Atlas simulator has been used and the models which are considered in this process are nonlocal band-to-band tunneling (BTBT) model and band gap narrowing (BGN) model [20, 30–33], Shockley-Read-Hall Recombination and Auger recombination [33, 34]. Trap-assisted tunnelling (TAT) model [34, 35], quantum confinement model (Hansch's Model) [33–35] is also considered. For mathematical solution Wentzel–Kramer–Brillouin approximation [34, 35] is considered to calculate tunneling probability. Models accuracy has been verified by reproducing the already reported Dielectric Modulated FET (DMFET) biosensor based experimental data [36] using the development platform of current work as shown in Fig. 1. Initially, DMTFET is tested for 400 nm nanogap length at low-k dielectric values and then its length has been reduced upto 100 nm and tested for different dielectrics. It has been found that simulated results nicely matched with the experimental results as shown in Fig. 2.

3 Results and discussions

In this section, we have shown the variation of dielectric ($K = 5, 7, 9$)/charge density ($\rho = -1e11, -5e12, -1e14$) of biomolecules such as single strand of DNA which is non hybridized possess both the dielectric constant as well as charge [37, 38] in the cavity region to show the sensitivity of the C-TFET and HM-SE-TFET biosensor.
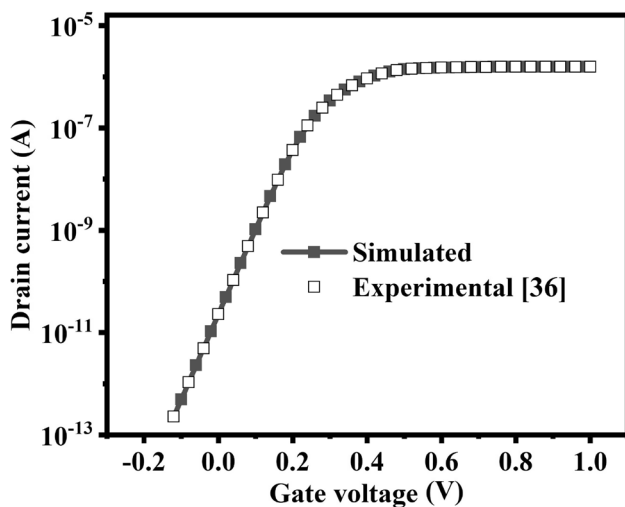
Fig. 2 Calibration with experimental results

3.1 Sensitivity analysis of a biosensor with dielectric variation in cavity region

In the proposed device, HM-SE-TFET, instead of using Si in the source region, SiGe has been used, which increases the steepness of the energy bands due to the lower energy band gap as compared to Si and Oxide used is high-κ compound HfO_2, for fine gate coupling. Further to this, an extra SE is deposited on the source region to accumulate the holes near the HfO_2/SiGe interface on the application of a negative potential to SE. This increases the abruptness at the source/channel junction. Due to this reason, the steepness of the energy band increasing with an increase in the dielectric constant of biomolecules, as the coupling strength of gate/channel increases as compare to conventional device i.e C-TFET, as shown in Fig. 3. The effect of dielectric variation of biomolecules are also reflected on surface potential as shown in Fig. 4a. Further, Fig. 4b shows the electric field at

Table 1 Parameter used for simulation

| Parameters	Symboles	C-TFET	HM-SE-TFET
Drain doping (cm^{-3})	N_D	1×10^{20}	1×10^{20}
Channel doping (cm^{-3})	N_D	1×10^{17}	1×10^{17}
Source doping (cm^{-3})	N_A	1×10^{20}	1×10^{20}
Drain length (nm)	L_D	100	100
Source length (nm)	L_S	100	100
Channel length (nm)	L_C	50	50
Silicon thickness (nm)	t_{si}	10	10
Oxide thickness (nm)	t_{ox}	6	6
Gate to Source electrode space (nm)	L_{SG}	–	8
Gate electrode work function (eV)	ϕ_G	4.5	4.5
Source electrode work function (eV)	ϕ_{SE}	–	4.5
Voltage at source electrode (V)	V_{SE}	–	– 1.2
Length of cavity (nm)	L_{Cavity}	15	30
Hight of cavity (nm)	t_{Cavity}	5.5	5.5
Fraction of Ge used in SiGe	–	–	0.5
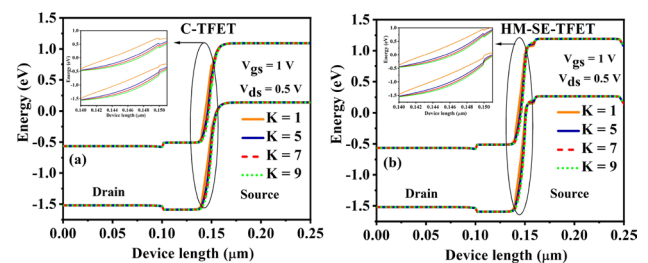
Fig. 3 Energy band diagram of **a** C-TFET and **b** HM-SE-TFET with different dielectric constants (K)
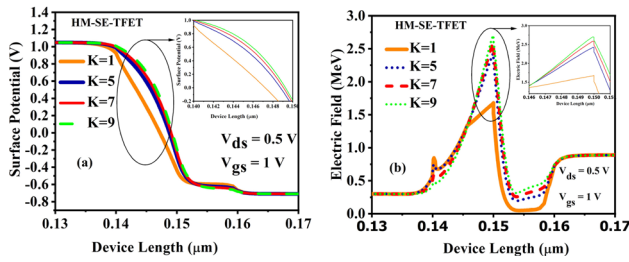
Fig. 4 **a** Surface potential and **b** electric field with different dielectric constants (*K*) of HM-SE-TFET
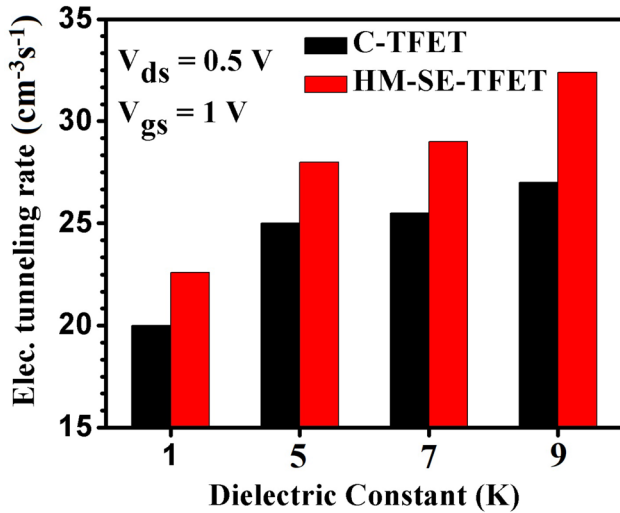

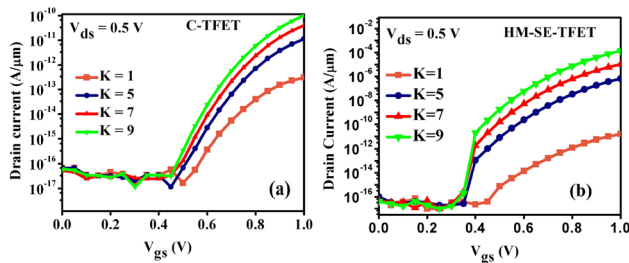**Fig. 5** Electron (e⁻) tunneling rate with different dielectric constants (*K*) of C-TFET and HM-SE-TFET

Fig. 6 I_{ds}–V_{gs} characteristics of **a** C-TFET and **b** HM-SE-TFET with different dielectric constants (*K*)

Fig. 7 I_{ds}–V_{ds} characteristics of **a** C-TFET and **b** HM-SE-TFET with different dielectric constants (*K*)

Fig. 8 Characteristics of I_{ds}–V_{gs} sensitivity of **a** C-TFET and **b** HM-SE-TFET with different dielectric constants (*K*)

Fig. 9 I_{ds}–V_{ds} sensitivity of **a** C-TFET and **b** HM-SE-TFET with different dielectric constants (*K*)

the source/channel junction and because of proposed modification a sharp peak is observed at the interface of source/channel junction, which is helpful for tunneling the charge carriers, hence the tunneling rate of the electron increases as the dielectric constant increases and it is much higher for the proposed device as compare to C-TFET as depicted in Fig. 5. Furthermore, for comparative picture of the effect of dielectric change in the cavity region Fig. 6a, b shows I_{ds}
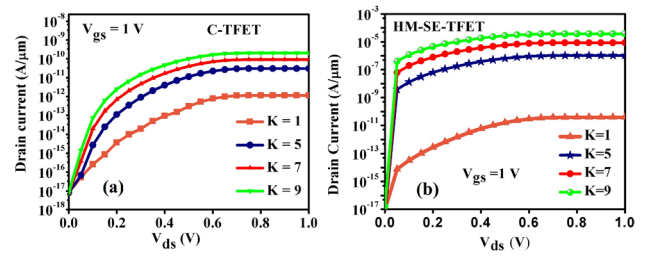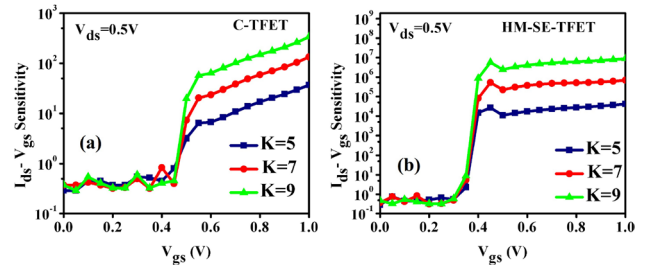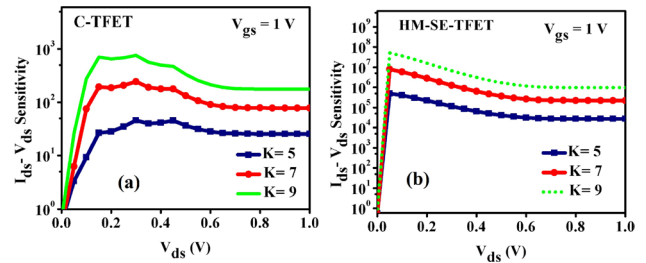
–V_{gs} and Fig. 7a, b shows I_{ds}–V_{ds} characteristics of C-TFET and HM-SE-TFET. Here it can be inferred that the change in I_{ds} w.r.t V_{gs} and V_{ds} is more in HM-SE-TFET biosensor in comparison to C-TFET biosensor.

The sensitivity of the biosensor is calculated as

$$S_{I_{ds}} = \left(\frac{I_{D,bio} - I_{D,air}}{I_{D,air}} \right) \tag{1}$$

Thus, Figs. 8 and 9 shows the sensitivity of HM-SE-TFET is higher as compare to C-TFET biosensor. The HM-SE-TFET sensitivity range is 10^4–10^7 for input characteristics and 10^4–10^6 for output characteristics.

In the design of biosensor sensing speed is essential parameter and transient time is the deciding factor. Time required by the carriers to travel from source to drain is
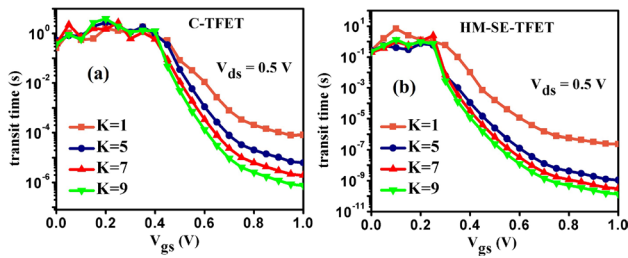
Fig. 10 Transit time(τ) of **a** C-TFET and **b** HM-SE-TFET with different dielectric constants (K)

Table 2 Comparison of sensing speed for different dielectric constants

Dielectric constants, K	Transient delay (s) of C-TFET	Transient delay (s) of HM-SE-TFET
1	8.0×10^{-5}	2.3×10^{-7}
5	6.2×10^{-6}	1.0×10^{-9}
7	1.9×10^{-6}	3.0×10^{-10}
9	7.5×10^{-7}	1.3×10^{-10}
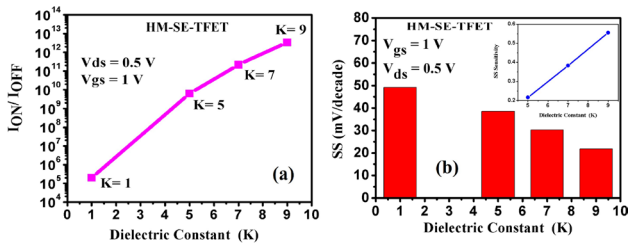
Fig. 11 **a** Plots of I_{ON}/I_{OFF} ratio and **b** SS and SS sensitivity with different dielectric constants (K) of HM-SE-TFET

called transient time and due to proposed modification abruptness at the junction is higher which provides a low transient delay as compared to C-TFET as shown in Fig. 10. Therefore, the proposed biosensor sensing speed is much higher as compared to the conventional biosensor are comprised in Table 2.

In addition to this, to show the impact of dielectric variation over device characteristics we have carried out ON state

to OFF state current ratio in Fig. 11a and SS in Fig. 11b. I_{ON}/I_{OFF} ratio increases while SS reduces with dielectric value. I_{ON}/I_{OFF} ratio is much affected than SS as dielectric changes. Therefore, it is proofed that proposed device has higher sensitivity in comparison to C-TFET biosensor and same can be verified from the comparison Table 3.

3.2 Sensitivity analysis of a biosensor with charge density variation in cavity region

In this manuscript, we have designed TFET based biosensor which can recognize both charge and neutral type of biomolecules in the cavity. To show sensitivity against the charge of biomolecules various electrostatic characteristics are carried out. Fig. 12a, b shows the energy band diagram of HM-SE-TFET and C-TFET for various charge densities. The presence of negative charges at extended cavity and Si/SiGe junction in HM-SE-TFET shows steeper band bending than C-TFET. Similarly, Fig. 13a, b capture surface potential and electric field range for HM-SE-TFET. Surface potential at the source channel interface which is mainly responsible for the tunneling of the charge carrier for conduction of the current. It is clearly understood that due to proposed modification large variation is observed in the electric field at the source/channel interface which will help to tunnel the charge carriers shown in Fig. 13b and to achieve a higher tunneling rate with a change in charge of the biomolecules present in the cavity region as depicted in Fig. 14. It also illustrates that tunneling rate for HM-SE-TFET is much higher than C-TFET.

The similar trends can be observed in the other parameters such as I_{ds}–V_{gs} characteristics which are shown in Fig. 15a, b, here, 10^{-12}–10^{-6} range of I_{ds} is measured with the varying charge of biomolecules in HM-SE-TFET and the output characteristics of the HM-SE-TFET device where the large deviation (10^{-13}–10^{-6}) is observed as compared to C-TFET as depicted in Fig. 16a, b, which can be easily reconciled. For showing superiority for HM-SE-TFET over C-TFET we have carried out input/output sensitivity of the device. I_{ds}–V_{gs} and I_{ds}–V_{ds} sensitivity in both cases as depicted in Figs. 17a, b and 18a, b respectively. HM-SE-TFET sensitivity is in the range of 10^6 which is large enough to identify which type of charged biomolecules are present in the cavity region as compare to C-TFET.

Table 3 Comparison of sensitivity for different dielectric constants

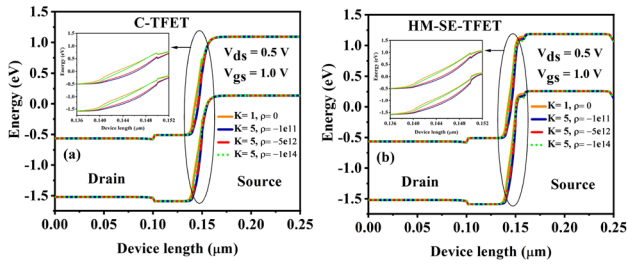| Dielectric constants, K	C-TFET		HM-SE-TFET	
	I_{ds}–V_{gs} sensitivity	I_{ds}–V_{ds} sensitivity	I_{ds}–V_{gs} sensitivity	I_{ds}–V_{ds} sensitivity
5	3.6×10^1	2.5×10^1	4.1×10^4	2.73×10^4
7	1.33×10^2	7.8×10^1	6.8×10^5	2.24×10^5
9	3.36×10^2	1.77×10^2	8.8×10^6	9.85×10^5

Fig. 12 Energy band diagram of **a** C-TFET and **b** HM-SE-TFET with negative charge density (ρ)
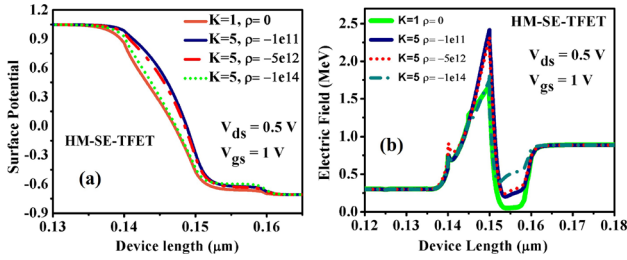

Fig. 13 a Surface potential and **b** electric field with negative charge density (ρ) of HM-SE-TFET
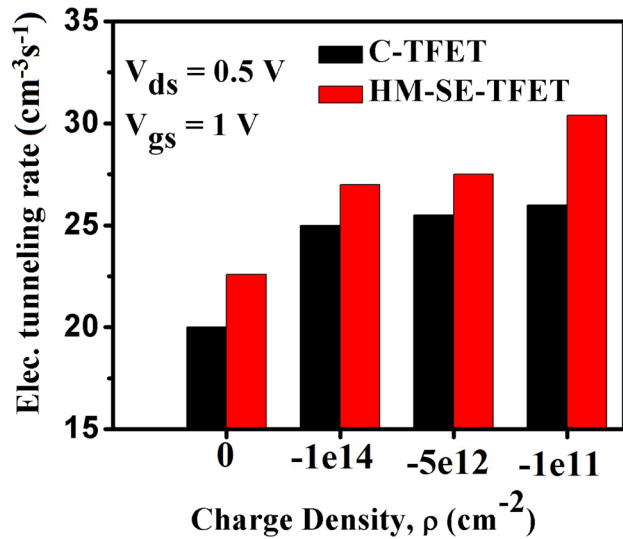

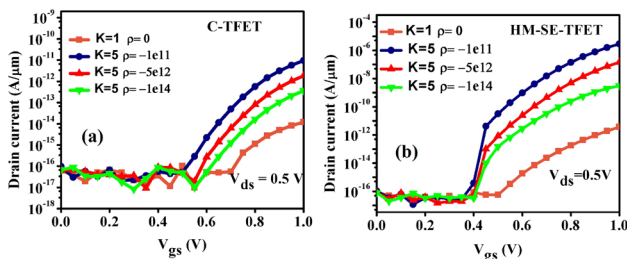**Fig. 14** Electron (e^-) tunneling rate with negative charge density (ρ) of C-TFET and HM-SE-TFET

Fig. 15 I_{ds}–V_{gs} characteristics of **a** C-TFET and **b** HM-SE-TFET with negative charge density (ρ)
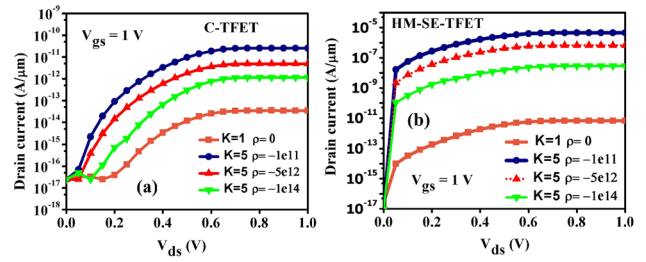

Fig. 16 I_{ds}–V_{ds} characteristics of **a** C-TFET and **b** HM-SE-TFET with negative charge density (ρ)
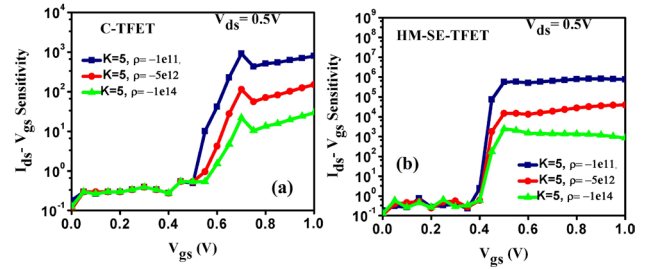

Fig. 17 Characteristics of I_{ds}–V_{gs} sensitivity of **a** C-TFET and **b** HM-SE-TFET with negative charge density (ρ)
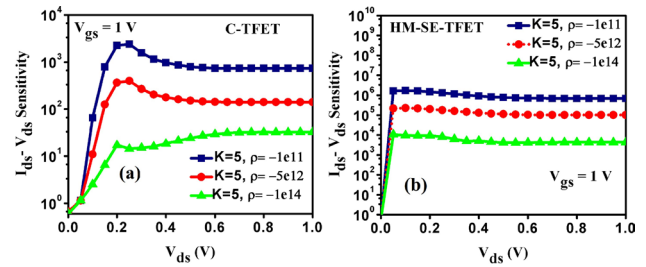
Fig. 18 I_{ds}–V_{ds} sensitivity of **a** C-TFET and **b** HM-SE-TFET with negative charge density (ρ)

Fig. 19 a Plots of I_{ON} / I_{OFF} ratio and **b** SS and SS sensitivity with negative charge density (ρ) of HM-SE-TFET
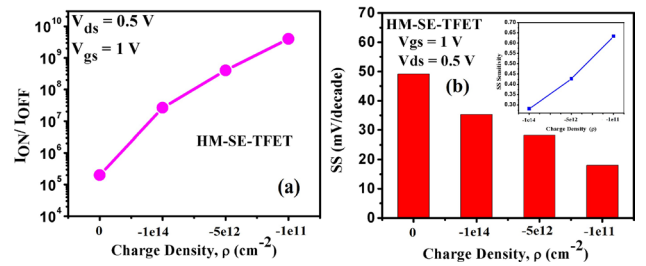
Finally, Fig. 19 showing device sensitivity in terms of ON-OFF current ratio and SS with the variation of the charges in the cavity. I_{ON}/I_{OFF} ratio increases and SS decreases with decreasing negative charge density. The

Table 4 Comparison of sensitivity for different charge densities

Charge density, ρ (cm^{-2})	C-TFET		HM-SE-TFET	
	I_{ds}–V_{gs} sensitivity	I_{ds}–V_{ds} sensitivity	I_{ds}–V_{gs} sensitivity	I_{ds}–V_{ds} sensitivity
-1×10^{11}	0.79×10^3	7.43×10^2	7.6×10^5	6.87×10^5
-5×10^{12}	1.51×10^2	1.41×10^2	3.9×10^4	1.00×10^5
-1×10^{14}	2.94×10^1	3.25×10^1	8.49×10^3	4.33×10^3

impact of charge density variation is more on I_{ON}/I_{OFF} ratio is more than SS. Hence, from the above mention discussion it can be understood that in the presence of charged biomolecules HM-SE-TFET shows higher sensitivity in comparison to C-TFET biosensor for this a summarized sensitivity is depicted in Table 4.

4 Conclusion

Proposed TFET-based biosensor has higher sensing speed in comparison to C-TFET biosensor, due to the modification at the source region. Hetero material provide low energy band gap and additional source electrode provides abruptness at the source/channel junction. Additional electrode overcome the material solubility limit and extension of cavity is helpful in making device more sensitive toward the biomolecules present in the cavity region.

References

1. M. Barbaro, A. Bonfiglio, L. Raffo, charge-modulated FET for detection of biomolecular processes: conception, modeling, and simulation. IEEE Trans. Electron Devices **53**(1), 158–166 (2006)
2. C.-H. Kim, C. Jung, H.G. Park, Y.-K. Choi, Novel dielectric modulated field-effect transistor for label-free DNA detection. Biochip J. **2**(2), 127–134 (2008)
3. J.Y. Kim, J.H. Ahn, S.J. Choi, M. Im, S. Kim, J.P. Duarte, C.H. Kim, T.J. Park, S.Y. Lee, Y.K. Choi, An underlap channel-embedded field-effect transistor for biosensor application in watery and dry environment. IEEE Trans. Nanotechnol. **11**(2), 390–394 (2012)
4. X.P.A. Gao, G. Zheng, C.M. Lieber, Subthreshold regime has the optimal sensitivity for nanowire FET biosensors. Nano Lett. **10**(2), 547–552 (2010)
5. N. Kannan, M.J. Kumar, Dielectric-modulated impact-ionization MOS transistor as a label-free biosensor. IEEE Trans. Electron Devices **34**(12), 1575–1577 (2013)
6. H. Im, X.-J. Huang, B. Gu, Y.-K. Choi, A dielectric-modulated field-effect transistor for biosensing. Nat. Nanotechnol. **2**, 430–434 (2007)
7. R. Gautam, M. Saxena, R.S. Gupta, M. Gupta, Numerical model of gate-all-around MOSFET with vacuum gate dielectric for biomolecule detection. IEEE Electron. Device Lett. **33**(12), 1756–1758 (2012)
8. R. Narang, M. Saxena, M. Gupta, Comparative analysis of dielectric-modulated FET and TFET-based biosensor. IEEE Trans. Electron. Devices **14**(3), 427–435 (2015)
9. S. Kanungo, S. Chattopadhyay, P.S. Gupta, H. Rahaman, Comparative performance analysis of the dielectrically modulated full-gate and short-gate tunnel FET-based biosensors. IEEE Trans. Electron. Devices **62**(3), 994–1001 (2015)
10. R. Narang, K.V.S. Reddy, M. Saxena, R.S. Gupta, M. Gupta, A dielectric-modulated tunnel-FET-based biosensor for label-free detection: analytical modeling study and sensitivity analysis. IEEE Trans. Electron. Devices **59**(10), 2809–2817 (2012)
11. K. Boucart, A.M. Ionescu, Double-gate tunnel FET with high-gate dielectric. IEEE Trans. Electron. Devices **54**(7), 1725–1733 (2007)
12. R. Narang, M. Saxena, R.S. Gupta, M. Gupta, Dielectric modulated tunnel field-effect transistor A biomolecule sensor. IEEE Electron Device Lett. **33**(2), 266–268 (2012)
13. R. Narang, K.V.S. Reddy, M. Saxena, R.S. Gupta, M. Gupta, A dielectric-modulated tunnel-FET-based biosensor for label-free detection: analytical modeling study and sensitivity analysis. IEEE Trans. Electron. Devices **59**(10), 2809–2817 (2012)
14. S. Kanungo, S. Chattopadhyay, P.S. Gupta, K. Sinha, H. Rahaman, Study and analysis of the effects of SiGe source and pocket-doped channel on sensing performance of dielectrically modulated tunnel FET-based biosensors. IEEE Trans. Electron. Devices **63**(6), 2589–2596 (2016)
15. D. Sarkar, K. Banerjee, Proposal for tunnel-field-effect-transistor as ultra-sensitive and label-free biosensors. Appl. Phys. Lett. **100**, 143108-1–143108-4 (2012)
16. M. Lanuzza, S. Strangio, F. Crupi, P. Palestri, D. Esseni, Mixed tunnel FET/MOSFET level shifters: a new proposal to extend the tunnel FET application domain. IEEE Trans. Electron. Devices **62**(12), 3973–3979 (2015)
17. S. Saurabh, M.J. Kumar, Novel attributes of a dual material gate nanoscale tunnel field-effect transistor. IEEE Trans. Electron Devices **58**(2), 404–410 (2010)
18. Mukta Singh Parihar and Abhinav Kranti, Enhanced sensitivity of double gate junctionless transistor architecture for biosensing applications. Nanotechnology **26**(14), 1–8 (2015)
19. M. Verma, S. Tirkey, S. Yadav, D. Sharma, D.S. Yadav, Performance Assessment of A Novel Vertical Dielectrically Modulated TFET-Based Biosensor. IEEE Trans. Electron Devices **63**(9), 3841–3848 (2017)
20. D. Singh, S. Pandey, K. Nigam, D. Sharma, D.S. Yadav, P. Kondekar, A charge-plasma-based dielectric-modulated junctionless TFET for biosensor label-free detection. IEEE Electron Devices Lett. **64**(1), 271–278 (2017)
21. S. Zhang, R. Geryak, J. Geldmeier, S. Kim, V.V. Tsukruk, Synthesis, assembly, and applications of hybrid nanostructures for biosensing. Chem. Rev. **117**, 12942–13038 (2017)
22. B. Wang, J.C. Cancilla, J.S. Torrecilla, H. Haick, artificial sensing intelligence with silicon nanowires for ultraselective detection in the gas phase. Nano Lett. **20**, 933–938 (2014)
23. D. Soni, D. Sharma, S. Yadav, M. Aslam, N. Sharma, Performance improvement of doped TFET by using plasma formation concept. Superlatt. Microstruct. **113**, 97–109 (2018)

24. C. Rajan, D. Sharma, D.P. Samajdar, Implementation of physical unclonable functions using hetero junction based GAA TFET. Superlatt. Microstruct. **126**, 72–82 (2019)

25. T. Poiroux, M. Vinet, O. Faynot, J. Widiez, J. Lolivier, T. Ernst, B. Previtali, S. Deleonibus, Multiple gate devices: advantages and challenges. Microelectron. Eng. **80**, 378–385 (2005)

26. X. Huang, W.-C. Lee, C. Kuo, D. Hisamoto, L. Chang, J. Kedzierski, E. Anderson et al. Sub 50-nm finfet: Pmos. *In International Electron Devices Meeting 1999. Technical Digest* (Cat. No. 99CH36318), pp. 67–70. IEEE (1999)

27. N. Lindert, L. Chang, Y.-K. Choi, E.H. Anderson, W.-C. Lee, T.-J. King, J. Bokor, H. Chenming, Sub-60-nm quasi-planar FinFETs fabricated using a simplified process. IEEE Electron Device Lett. **22**(10), 487–489 (2001)

28. C., Jean-Pierre, M.H. Gao, A. Romano-Rodriguez, H. Maes, C. Claeys. Silicon-on-insulator'gate-all-around device. In: *International Technical Digest on Electron Devices*, pp. 595–598. IEEE (1990)

29. Z., Ming, S.S. Tan, E.H. Toh, E. Quek. Method of fabricating a silicon tunneling field effect transistor (TFET) with high drive current. U.S. Patent 8,368,127, issued February 5, (2013)

30. K. Kalantar-Zadeh, K.J. Berean, N. Ha, A.F. Chrimes et al., A human pilot trial of ingestible electronic capsules capable of sensing different gases in the gut. Nat. Electron. **1**, 79–87 (2018)

31. K. Kalantar-Zadeh, C.K. Yao, K.J. Berean, N. Ha et al., Intestinal gas capsules: a proof-of-concept demonstration. Gastroenterology **150**, 37–39 (2016)

32. S. Kanungo, S. Chattopadhyay, P.S. Gupta, H.H. Rahaman, Comparative performance analysis of the dielectrically modulated full gate and short-gate tunnel FET-based biosensors. IEEE Trans. Electron Devices **62**(3), 994–1001 (2015)

33. ATLAS device simulation soft, Silvaco, Santa Clara, CA, USA (2012)

34. J.L. Padilla, F. Gamiz, A. Godoy, Impact of quantum confinement on gate threshold voltage and subthreshold swings in double-gate tunnel FETs. IEEE Trans. Electron Devices **59**(12), 3205–3211 (2012)

35. W. Hansch, T. Vogelsang, R. Kircher, M. Orlowski, Carrier transport near the Si/SiO2 interface of a MOSFET. Solid State Electron. **32**(10), 839–849 (1989)

36. H. Im, X.-J. Huang, G. Bonsang, Y.-K. Choi, A dielectric-modulated field-effect transistor for biosensing. Nat. Nanotechnol. **2**(7), 430 (2007)

37. C.-H. Kim, C. Jung, H.G. Park, Y.-K. Choi, Novel dielectric modulated field-effect transistor for label-free DNA detection. Biochip J. **2**(2), 127–134 (2008)

38. A. Offenhusser, R. Rinaldi, *NanobioelectronicsFor Electronics, Biology, and Medicine* (Springer, New York, 2009)